Paper No.
66—WA/HT-24

R. N. MERONEY
Assistant Professor of Civil Engineering,
Colorado State University,
Fort Collins, Colo.

W. H. GIEDT
Professor of Mechanical Engineering,
University of California,
Davis, Calif.

The Effect of Mass Injection on Heat Transfer From a Partially Dissociated Gas Stream[1]

An investigation of the effect of hydrogen and helium injection on local heat transfer to a porous surface from an oxygen-acetylene combustion gas stream is described. The free-stream temperature varied from 6200 to 5200 deg Rankine and the volumetric percentage of atomic hydrogen from 20 to 8. Flow in the boundary layer was found to be turbulent. Study of the results led to successful correlation of the ratio of the heat flux with injection to the heat flux without injection in terms of a dimensionless blowing parameter in which properties are evaluated at an average reference state. A method for predicting heat flux with injection was then developed. This is based on a temperature rather than an enthalpy potential because the latter resulted in anomalous values for the Stanton number under some of the test conditions.

Introduction

THE effectiveness of transpiration in reducing heat transfer from a high-temperature gas stream has been the subject of many experimental and analytical studies. Gas injection into laminar boundary layers has received greater attention because it is amenable to analytical solution [1, 2, 3, and 4].[2] In most applications, however, flow in the boundary layer is turbulent. In fact, with injection turbulent boundary layers are more likely to prevail even at low Reynolds numbers because turbulence level in high-temperature gas streams is frequently high, permeable walls are inherently rough, and continuous injection has a destabilizing effect on boundary-layer flow. Lack of knowledge concerning turbulent exchange mechanisms has severely limited solution of the differential equations governing turbulent boundary-layer flow.

Numerous investigators have made analyses and performed experiments to determine the effect of distributed air transpiration through a flat surface parallel to an air stream for which the flow in the boundary layer is turbulent [2, 5, 6, 7]. Results show that both skin friction and heat transfer are reduced, but less than in a laminar boundary layer. It is also known that injection of a light molecular weight gas into the boundary layer is more effective than air in reducing the magnitude of the heat or momentum exchange with the wall surface [8–14].

There is relatively little experimental turbulent boundary-layer data with mass transfer. In particular there have been no successful integrated studies of heat, mass, and momentum transfer. Also very little data exists for the environmental extremes of temperature, heat transfer rate, and possible chemical reactions which occur under these conditions. Most laboratory data is in the range of low ambient temperature and moderate heat flux rates, which can often mask characteristics that are critical in actual applications.

With these thoughts as impetus an experimental program was outlined to obtain heat transfer rates to a flat plate from a dissociated turbulent boundary layer into which light molecular

[1] Use of experimental apparatus developed for the NASA Marshall Space Flight Center under Contract NAS 8-850 is gratefully acknowledged.

[2] Numbers in brackets designate References at end of paper.

Contributed by the Heat Transfer Division for presentation at the Winter Annual Meeting, New York, N. Y., November 27–December 1, 1966, of THE AMERICAN SOCIETY OF MECHANICAL ENGINEERS. Manuscript received by Heat Transfer Division July 9, 1965; revised manuscript received July 7, 1966. Paper No. 66—WA/HT-24.

Nomenclature

A = slope of surface temperature history, equation (6)
b = parameter, equation (13)
C_f = skin friction coefficient
C_H = Stanton number, $q/\rho u c_p(T_e - T_w)$
c = specific heat capacity
c_p = specific heat capacity at constant pressure
D_{iM} = diffusion coefficient of component i with respect to mixture
D_{ij} = binary diffusion coefficient of species i through j
F = blowing parameter, $F = (\rho_w v_w)/(\rho_e u_e)$
F^* = blowing parameter based on reference state, $F^* = (\rho_w v_w)/(\rho^* u_e)$
g = gravitational constant
h = sensible enthalpy, $h = \int_0^T c_p dT$
h^0 = enthalpy of formation
H = total enthalpy, $H = \int_0^T c_p dT + h^0 + u^2/2g$
k = thermal conductivity
L = plate length
Le = Lewis number, $D\rho c_p/k$
M = molecular weight
p = pressure
Pr = Prandtl number, $\mu c_p/k$
q = local heat transfer rate per unit area
r_0 = recovery factor
R = universal gas constant
Re = Reynolds number, $u_e x \rho_e/\mu_e$
t = time
T = temperature
u, v = stream velocity parallel and perpendicular to plate
w = width
x = distance along plate
y = distance normal to plate
z = plate thickness
α = thermal diffusivity
δ = boundary-layer thickness
ϵ = emissivity
ϵ_k = turbulent eddy conductivity coefficient
ϵ_D = turbulent eddy diffusivity coefficient
μ = absolute viscosity
ρ = density
σ = Stefan-Boltzmann constant
ω = mass fraction

Subscripts

a = mixture components other than those components added at wall
aw = adiabatic wall
c = convective
cb = ceramic brick

(Continued on next page)

Discussion on this paper will be accepted at ASME Headquarters until January 9, 1967

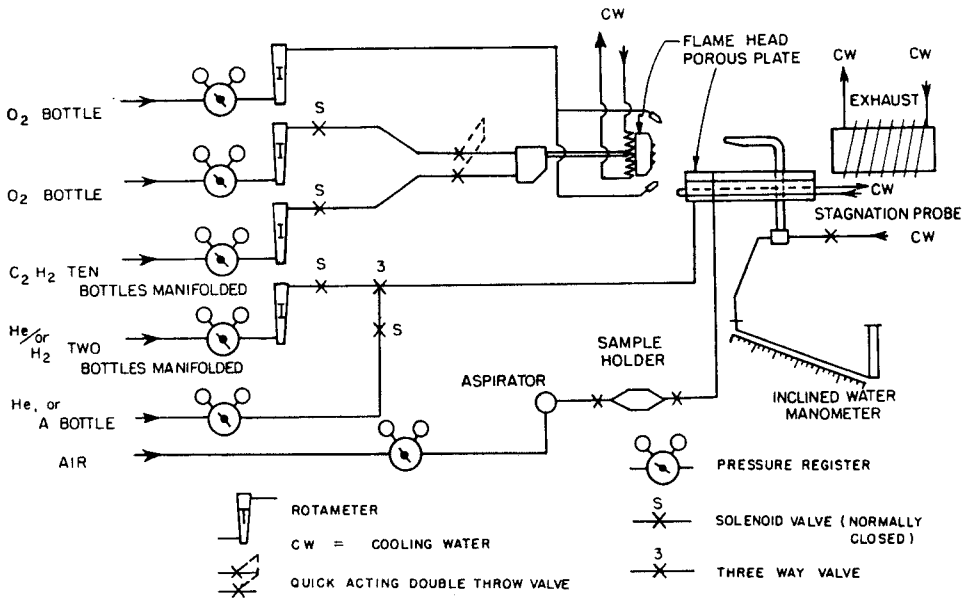

Fig. 1 Oxyacetylene flame head, porous plate, and supporting equipment

weight gases could be injected [15]. The free-stream medium chosen was an oxygen-acetylene flame containing an appreciable percentage of dissociated hydrogen. Hydrogen and helium were injected through a porous stainless-steel test section held parallel to the combustion gas flow. As a second phase to this investigation a method was developed to predict heat transfer for this type of system. This was based (1) on correlation of the ratio of the heat flux with injection to the heat flux without injection as a function of a dimensionless parameter which incorporated the wide variations owing to Reynolds number, foreign gas injected, and wall to free-stream temperature ratio; and (2) on a relation for heat transfer from a reactive turbulent boundary layer without mass transfer to use with the experimental curve of the heat flux ratio. This is discussed after a description of the experimental procedure and results.

Experimental Equipment and Procedure

The test apparatus (see Figs. 1 and 2) consisted of a multiple nozzle oxygen-acetylene flame head, a mass transfer section, and exhaust duct. The equipment was so designed that when oxygen and acetylene were passed through the flame head and burned a two-dimensional high-temperature gas stream was produced which provided parallel flow heating to a 3 × 6-in. test area. The average nonblowing heating rate was approximately 40 Btu/ft² sec. The free-stream gas velocity was approximately 200 ft/sec with a temperature of about 5000 deg F at atmospheric pressure.

Transpiration Test Section. The transpiration surface consisted of a 3 × 6-in. × 1/4-in-thick plate of AISI 316 porous stainless steel. The mean pore size was 20 microns with a mean particle dia of 65 microns. As shown in Fig. 3, this plate formed the upper wall of a plenum chamber to which the injected gas was

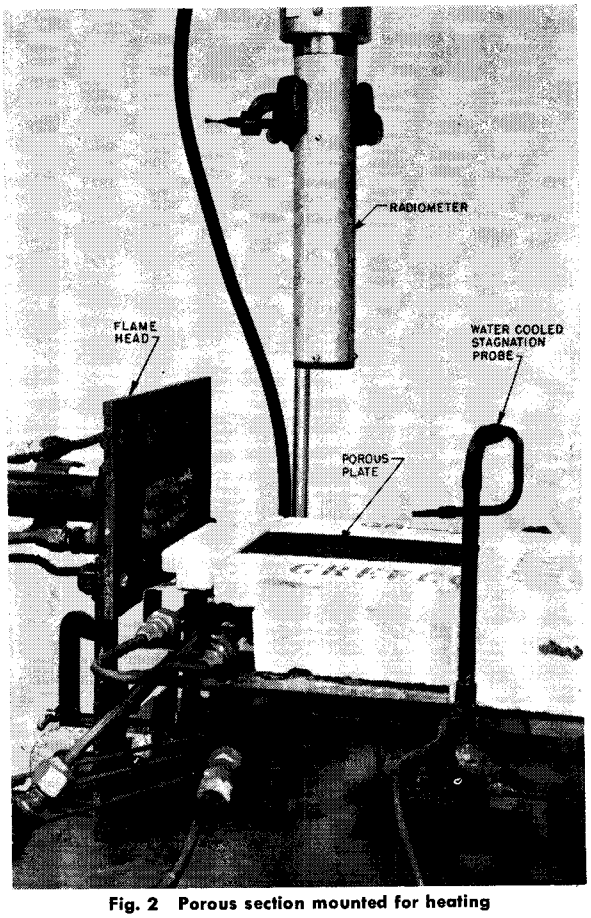

Fig. 2 Porous section mounted for heating

Nomenclature

cp = calorimeter plate
e = free-steam value
g = free-steam gas
i = species
j = injected gas species
k = conduction
l = lower surface of plate
m = mean value in vertical direction between upper and lower surfaces
M = mixture
o = no blowing
p = plenum chamber
r = radiative
s = stagnation conditions
t = transpiration coolant
u = upper surface of plate
w = heated surface and porous plate
∞ = surrounds

Superscripts

$( )'$ = no chemical reaction occurs, equation 10
$( )^*$ = reference temperature state
$(\overline{\ })$ = mixture

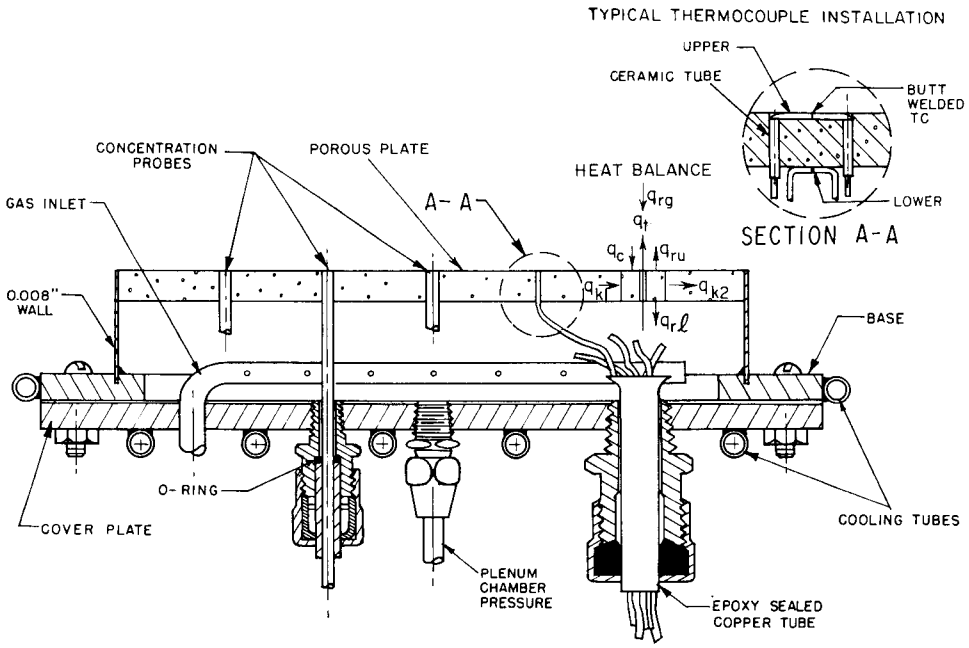

Fig. 3 Porous plate and instrumentation

supplied. The side walls of the chamber (cut from 0.008-in-thick AISI 304 stainless-steel shim stock) were copper and nickel-gold brazed to the porous plate and silver-soldered to a copper base plate. The lower side of the plenum chamber was cooled with water coils. Seven chromel-alumel thermocouples were butt-welded and mounted in 0.016 × 0.016-in. slots in the upper surface of the plate at locations 1/4, 1/2, 1, 2, 3, 4, and 5 in. from the leading edge. Seven thermocouples were spot-welded at similar locations along the bottom of the plate (see insert in Fig. 3). Care was taken to orient each thermocouple in an isothermal line normal to the flow direction. Small (0.032-in. OD) ceramic tubing electrically insulated the upper thermocouple lead wires from the plate. The tubes were held in place with ceramic cement which had a maximum service temperature of 4300 deg F. Three 1/8-in-OD stainless-steel surface concentration probe tubes were force-fitted into the porous plate, brought through the chamber, and sealed with fittings (shown in Fig. 3). Injected gas was supplied through a 1/8-in-ID copper tube drilled to distribute the gas along the length of the plenum chamber. The chamber was also instrumented to measure the coolant gas temperature and pressure.

Convective Heat Transfer Distribution. Test records provided a set of steady-state temperature readings, injected gas mass flow rates, and total radiation radiometer readings. The local convective heat flux to the plate was determined from the following energy balance on small elements at each thermocouple location (see Fig. 3):

$$q_c = q_t + q_{ru} + q_{rl} + q_{k1} - q_{k2} - q_{rg} \tag{1}$$

where q_c is the heat transferred from the boundary layer by conductive and diffusive mechanisms in the gas; q_{ru} and q_{rl} are the radiative heat rates from the upper and lower surfaces of the plate; q_t represents the increase in sensible heat of the injected gas; q_{k1} and q_{k2} are the rates at which heat is conducted into and out of the element in the direction along the plate; and q_{rg} is the radiation heat rate from the gas to the plate surface. Substitution of appropriate expressions for the individual heat rates yields

$$q_c = [\rho v(h(T_{wu}) - h(T_p))]_t + \epsilon_w\sigma(T_{wu}^4 + T_{wl}^4 - 2T_\infty^4) - k_w z_w \left(\frac{d^2T}{dx^2}\right)_m - \epsilon_g T_g^4 \tag{2}$$

for the local convective heat rate. Water cooling of the test section base plate, and the low absorptivity of this gas (~0.001) and short path length through the gas justified approximating the temperature of the surroundings as T_∞ for radiation from the upper and lower surfaces.

Studies of gas flow through a plane wall of porous material have established the following relationship between mass flow rate and the several governing parameters [16]:

$$\left(\frac{\rho v}{\mu}\right)_t \sim \left(\frac{p_{wl}^2 - p_{wu}^2}{\mu_t^2 T_m}\right)^{1/2} \tag{3}$$

Since the pressure difference across the porous section may be assumed constant, variations in local mass flow rate depend on inverse square root of local mean wall temperature. It is convenient to express the local mass injection rate as

$$(\rho v)_{tx} = (\rho v)_{tL}\left(\frac{T_{mL}}{T_{mx}}\right)^{1/2} \tag{4}$$

where $(\rho v)_{tL}$ is equal to

$$(\rho v)_{tL} = \frac{G}{w\int_0^L \left(\frac{T_{mL}}{T_{mx}}\right)^{1/2} dx}$$

and

G = total mass flow of coolant lbm/sec
w = width of porous section
T_{mL} = mean wall temperature at trailing edge of porous section
T_{mx} = local mean wall temperature

The thermal conductivity of the porous stainless-steel plate was calculated from the thermal diffusivity, α. The variation of α with temperature was measured by a transient technique [15]. The resulting variation was essentially linear and could be represented by $\alpha = 0.032 + 0.000045T$ from room temperature up to 1800 deg R (T in deg R and α in ft²/hr). The plate density was measured, and the specific heat capacity at mean plate temperatures was taken from reference [17].

Velocity, Flame Temperature, and Wall Concentration Measurements. A water-cooled impact probe consisting of a 1/6-in-OD tube surrounded by a 1/4-in-OD copper water jacket was designed to measure velocity profiles through the boundary layer. Static

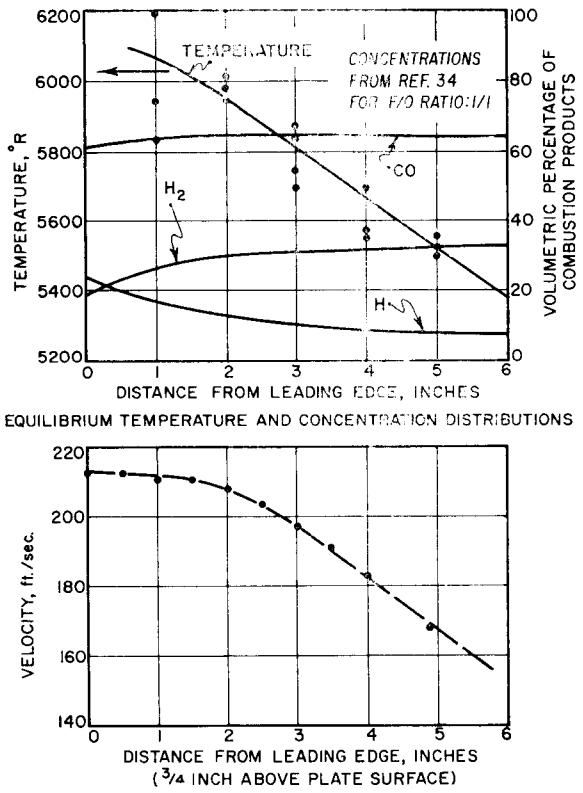

Fig. 4 Temperature, concentration, and velocity distributions along center line of test section

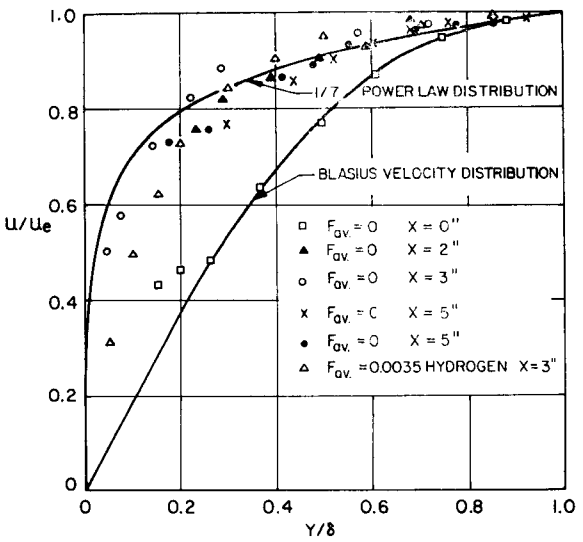

Fig. 5 Typical velocity profiles

pressure measurements indicated that atmospheric pressure conditions existed across the flame. Stagnation measurements were made at 1-in. intervals along the plate from the surface to midstream in 0.025-in. increments. Free-stream velocities are plotted versus plate position in Fig. 4. Typical boundary-layer velocity profiles for blowing and nonblowing conditions are plotted in Fig. 5 and depict the turbulent character of the flow.

Because of the low Mach number of the flow the velocity could be related to the impact pressure rise by the Bernoulli equation. To evaluate the density the temperature and velocity profiles were assumed to be similar. This assumption combined with the perfect gas law yields the following equation:

$$u = \left[\frac{gR(T_e - T_{wu})(p_s - p_\infty)}{Mu_e p_\infty}\right] + \left[\left(\frac{gR(T_e - T_{wu})(p_s - p_\infty)}{Mu_e p_\infty}\right)^2 + 2\left(\frac{R(p_s - p)gT_{wu}}{Mp_\infty}\right)\right]^{1/2} \quad (5)$$

The temperature in the gas stream was measured by the sodium line reversal technique. Details of the apparatus used are given in reference [15]. It is estimated that, with the extra precautions taken, the final results for flame temperature shown in Fig. 4 are accurate to ±150 deg R. The emissivity of the exhaust gas (considered to be gray) was approximately 0.001 (evaluated from radiometer measurements). Radiation from the gas to the plate was a maximum of two percent of the smallest heating rate.

To determine the net radiative heat flux away from the plate two mirror-type directional radiometers were positioned vertically over the apparatus. They viewed representative circles of about 1-in. in dia on the surface. Evaluation of the radiometer output for each run revealed an average total emissivity of 0.65. This value is of the order of magnitude predicted by Eckert, et al., for such a porous material [18].

Gas samples were analyzed with a chromatograph using nitrogen as a carrier gas. Details of the chromatograph calibration and operation may be found in Appendix B of reference [15].

Samples for analysis were obtained through stainless-steel probes incorporated into the apparatus. These were taken during the test runs after steady state had been reached, as indicated by the surface thermocouples. In order to insure a very weak suction which would not significantly affect the boundary layer an aspirator was used. Samples were removed from the probing system with a gastight hypodermic syringe and were stored in 8 cc evacuated medical serum bottles. The serum bottles remained gastight over extended periods of time and were completely satisfactory for transporting or storing containers.

Measurement of Zero-Transpiration Heat Rates. For determining the zero-transpiration heat rates to the wall surface an AISI 304 stainless-steel calorimeter plate (1/8 × 3 × 6 in.) was instrumented with six chromelalumel thermocouples located at positions 0.5, 1.5, 2.5, 3.5, 4.5, and 5.5. in. from the leading edge. This plate was mounted in the test section in place of the transpiration chamber and the thermocouple outputs recorded during transient heating. The local heat flux was calculated from the equation

$$q_0 = \left[\rho cz \frac{dT}{dt}\right]_{cp} + \left[\frac{2kAT}{\sqrt{\pi\alpha t}}\right]_{cb} + \epsilon_{cp}\sigma T_{cp}^4 - \epsilon_g \sigma T_g^4 - \left[kz\frac{d^2T}{dt^2}\right]_{cp} \quad (6)$$

where the first term denotes the rate of energy storage in the plate, the second the rate of heat loss from the lower surface to the ceramic brick on which the plate was mounted, the third the rate of radiation to the surroundings. The fourth and fifth terms, which are conduction and gaseous radiation corrections, respectively, were negligible.

Experimental Results

The possible range of mass transfer rates was determined by the maximum injection rate the boundary would withstand without separation[3] and the maximum temperature at which the brazed joints of the porous plenum chamber could be expected to remain intact. Data were taken for one helium and three hydrogen injection rates. The consistency of experimental results from run to run under the same transpiration condition was very satisfactory. Representative measurements of the flame side (upper) and the coolant gas side (lower) steady-state temperatures of the

[3] Determined experimentally by observing when the transient temperature rise of the plate was comparatively slow.

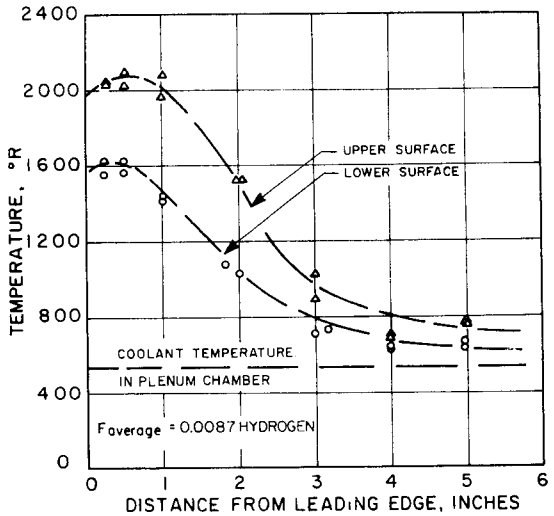

Fig. 6 Porous plate wall temperatures with hydrogen injection

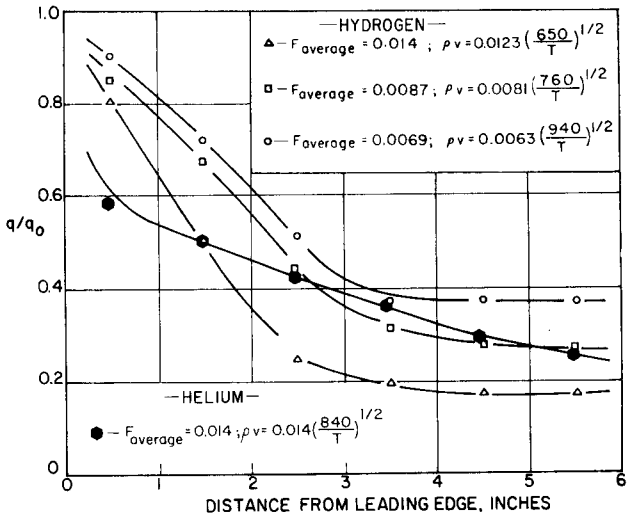

Fig. 7 Heat transfer ratio with hydrogen injection

porous plate are shown in Fig. 6. The effect of end losses to the forward plenum wall is evident. The uniformity of surface temperature normal to the flow direction in the center half of the plate had been confirmed previously [19].

Only the maximum transpiration rate of helium was studied because the steady-state temperatures of the porous plenum chamber were in the critical range. The local heat transfer rates to the wall were calculated by the procedure described previously. The ratio of these quantities to the no-transpiration heat rates obtained by a calorimeter plate (for the same surface temperature distribution) is plotted in Fig. 7 versus plate position. The average value of the blowing parameter F was 0.014; however, owing to the wall temperature variation, the actual local injection rates varied from 0.0098 at the leading edge to 0.0170 at the trailing edge of the porous stainless-steel plate. The injection of helium reduced the heat transfer ratio q/q_0 from 1.0 at the leading edge to 0.24 at the trailing edge of the test section.

Three transpiration conditions were studied with hydrogen injection. The average values of the blowing parameter were 0.014, 0.0087, and 0.0069. The actual injection ranges varied from 0.0109 to 0.0195, 0.00585 to 0.0113, and 0.00485 to 0.00876, respectively. The ratio of the local heat transfer rates to the local zero-transpiration values versus plate position are also plotted in Fig. 7. It is interesting that in each case the ratio of q to q_0 approaches a constant value at about the 4-in. location. These values depend on the transpiration rate and should be indicative of the value of q/q_0 which would apply to regions beyond 6 in. if the transpiration section were longer. The injection of hydrogen at $F = 0.014$ reduced the heat transfer ratio q/q_0 to an asymptotic value of 0.18. Hydrogen injection at $F = 0.0069$ reduced the heat transfer ratio to an asymptotic value of 0.37. Hence a 100 percent increase in blowing rate (from 0.0069 to 0.014) reduced the heat transfer ratio at the trailing edge by 100 percent also.

Discussion of Experimental Results and Suggested Heat Flux Prediction Procedure

The main objective of the theory of convective heat transfer is to make possible the calculation of the heat flux between a solid surface and fluid stream in contact with it for specified surface and flow conditions. The case of injection, however, is very complex when foreign gases and high temperatures are involved. At present, theory has not been developed for these conditions; hence, for design purposes, it is convenient to use experimental information concerning the variation of the heat flux ratio, q/q_0, as a function of a blowing parameter. This procedure makes the calculation of the nonblowing heat transfer very important. In the present study this involved consideration of the heat flux potential most appropriate under mass injection conditions.

Selection of Heat-Rate Potential The occurrence of chemical reactions in boundary-layer flow and specific heat capacity variation makes the use of an enthalpy potential advantageous. The complexity of the governing differential energy equation can be considerably reduced when written in terms of the enthalpy rather than the temperature for the case when the laminar and turbulent Lewis numbers are equal to 1.0 [20].

In the course of evaluation of the heat transfer measurements from the oxygen-acetylene combustion gas stream, however, it became evident that conditions can occur where the use of an enthalpy driving potential would yield misleading heat transfer coefficients. This is most likely to occur when a lightweight molecular gas is injected at the wall and when the dissociation energy in the free stream does not overshadow its sensible energy. For example, in the present experiment for convective heating without mass transfer, the free-stream Reynolds number was of the order of 20,000, the temperature potential 4800 deg R, and the enthalpy potential approximately $(H_e - H_w) = 3098$ Btu/lbm. At the same Reynolds number and temperature difference when the mass fraction of hydrogen at the wall was 0.8, the enthalpy potential was calculated to be $(H_e - H_w) = 500$ Btu/lbm. The measured value of q/q_0 for these conditions is 0.49. Writing $q/q_0 = (C_H)(H_e - H_w)(\rho u)_e/C_{H0}(H_e - H_w)_0(\rho u)_e$ and substituting the preceding values yields $C_H/C_{H0} = 3.0$. This result is attributable to the large difference between the specific heat capacities of the free stream and of the injected gas.

Since correlation of the heat transfer rates in terms of an enthalpy potential would involve unrealistic values for the ratio of the conductances, it was proposed that a temperature potential $(T_{aw} - T_w)$ be employed together with the specification of a reference temperature and composition at which properties are to be evaluated. This approach is developed in the following paragraphs.

Reactive Boundary Layer Without Mass Transform. Several authors have proposed modifications of the equations for incompressible boundary-layer heat transfer coefficients to account for the effect of chemical reaction, wall temperature variation, and fluid property variation. Rose, Probstein, and Adams [20] concluded that the various fluid properties should be evaluated at the free-stream state. They reasoned that large changes in density and other fluid properties occur in the laminar sublayer, but that, since the magnitude of the momentum in the sublayer is a small fraction of the total boundary-layer momentum, the overall growth of the momentum thickness should not be significantly influenced by the sublayer. Calculation of the heat flux rates for the conditions

of this experiment based on fluid properties of the free-stream state yielded values lower than those measured. This was attributed to the effect on fluid properties of the significant percentage of atomic hydrogen which existed in the free stream but not at the wall; also the large variations in temperature and concentration were probably not restricted to the laminar sublayer.

An alternate procedure is to evaluate properties at an appropriate reference state. In a recent review of this approach Knuth [22, 23] recommends the following expressions for the reference temperature and composition:

$$T^* = 0.5(T_w + T_e) + 0.2r_0 \frac{u_e^2}{2c_p^*}$$
$$\omega_i^* = \frac{\omega_{iw} + \omega_{ie}}{2} \tag{7}$$

The constant property heat-rate equations in which the foregoing values are to be used are for a laminar boundary layer,

$$q_{0_{\text{laminar}}}^* = 0.332 \frac{k^*}{x} \text{Re}_x^{*1/2} \text{Pr}^{*1/3} (T_{aw} - T_w) \tag{8}$$

and for a turbulent boundary layer,

$$q_{0_{\text{turbulent}}}^* = 0.0291 \rho^* c_p^* u_e (\text{Re}_x^*)^{-0.2} (\text{Pr}^*)^{-2/3} (T_{aw} - T_w) \tag{9}$$

These equations must also be modified to account for the effect of reactive species.

Investigations of reactive boundary-layer heat transfer have shown that diffusion and recombination of a dissociated species introduces a term involving the concentration potential multiplied by the diffusion coefficient. The expression utilized herein to account for the recombination of the atomic hydrogen found in the oxygen-acetylene combustion products is derived in the Appendix of this paper. It is[4]

$$\frac{q_0}{q_0'} = 1 + \frac{\sum_i \text{Le}^{*2/3} h_i^0 (\omega_{ie} - \omega_{iw})}{c_p^* (T_{aw} - T_w)} \tag{10}$$

Incorporating the experimental values for the local free-stream temperature and local velocity and the appropriate wall temperature distributions into equations (7) through (10) yielded the analytical curves for zero injection (labeled q_0) shown in Fig. 8 for the laminar and turbulent heat transfer conditions. Results for other injection rates were similar.

Note that the experimental heat transfer rates over the first half of the test surface conform closely to the predicted laminar heat transfer distribution. In the latter half they asymptotically approach the predicted values for a turbulent layer. This behavior indicates transition occurred in the midsection of the plate at Reynolds numbers of 10,000 to 15,000. Although these values may appear low, transition at similar values when reactions occur has been reported [24]. With mass injection into the boundary-layer turbulent flow over flat plates at Reynolds number values as low as 1678 have been observed [25]. Therefore, considering the character of the heat transfer and velocity profiles measured, it was concluded that the boundary layer over the test region during no-blowing was turbulent with the possible exception of the first 2 in. Mass injection would tend to move the transition region even further forward.

The validity of equation (9) for predicting heat transfer from a turbulent boundary layer has been well established in the Reynolds number range of 10^5 to 10^7. Present results suggest that it is applicable for values of Re down to 10^4.

Mass Fraction of Injected Species at Wall. Representative results for the mass fraction of hydrogen from the analyses of gas samples taken at the 1, 2, and 3-in. positions along the plate for the various runs are plotted in Fig. 9. The helium data also displayed lower values in the initial injection region and increase in the downstream direction. The need for more data is apparent.

[4] The range of q_0/q_0' predicted by equation (10) for the conditions of this experiment was from 1.35 to 2.2.

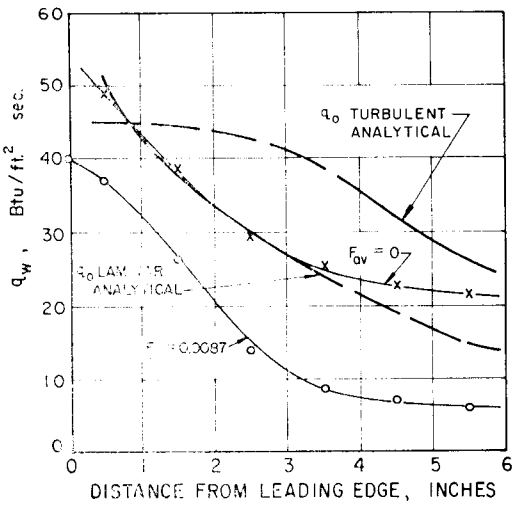

Fig. 8 Heat transfer rates at wall for hydrogen injection with F_{av} = 0.0087

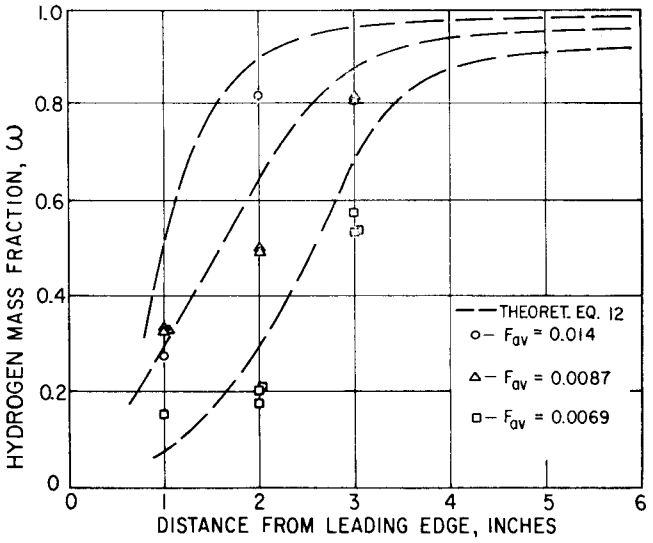

Fig. 9 Wall mass fraction with hydrogen injection

Romanenko and Kharchenko [26] derived an expression for wall concentration from (1) the formula for determination of the injected gas supply rate at the wall,

$$\rho_w v_w = \omega_w \rho_w v_w - \rho_w D_{jM} \left[\frac{d\omega_j}{dy} \right]_w \tag{11}$$

(2) the assumption of a simple Reynolds analogy, $C_f/2 = C_H \text{Pr}^{2/3}$, and (3) the assumption that the Schmidt number was unity. If their results are modified by allowing the Schmidt number to vary and introducing the concept of a reference state, a more general expression for wall concentration is obtained. It is

$$\omega_w = \frac{b}{1 + b} \tag{12}$$

where

$$b = \frac{\rho_w v_w}{\rho^* u_e} \frac{\text{Pr}^{*1/3}}{\text{Le}^*} \frac{1}{C_H^*} \tag{13}$$

The dashed lines in Fig. 9 represents wall mass fractions based on

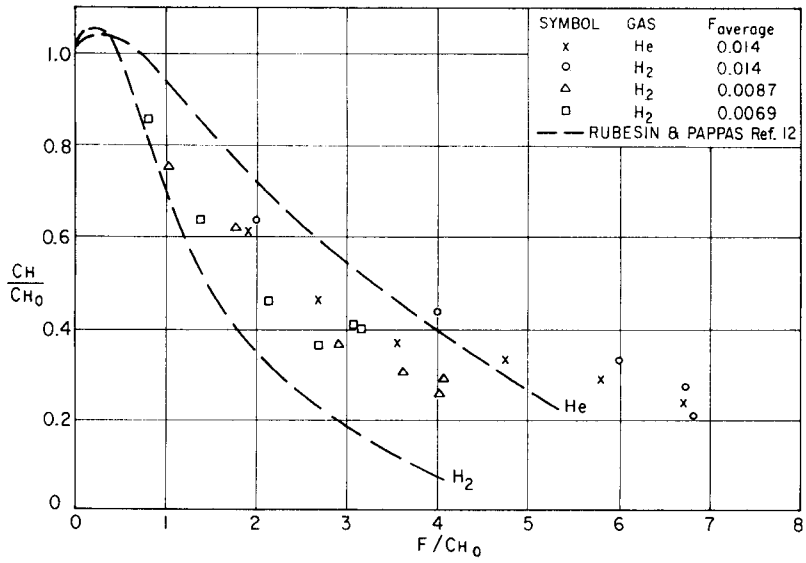

Fig. 10 Heat transfer ratio as a function of blowing parameter, F/C_{H0}

calculations using equations (12) and (13) and the experimental heat transfer results. Agreement between the curves and the experimental data is very good considering the difficulties involved in making measurements of this type. The data tends to fall somewhat below the analytical curves, which confirms the observation of Knuth, that sucking a gas sample through a hole in the wall measures a coolant concentration less than the wall concentration [21].

Correlation of Effect of Mass Injection on Heat Transfer

Present correlation techniques for turbulent boundary-layer heat transfer with injection are based upon dimensional analysis and extension of successful laminar boundary-layer results with mass transfer [4, 22, 27, 28]. A procedure which appears to have particular merit (e.g., see reference [30]) is to plot the ratio of the Stanton number for the heat flux rate in the presence of mass transfer to the Stanton number for the heat flux rates with zero injection versus the dimensionless injection rate, $F = (\rho_w v_w)/(\rho_e v_e)$, divided by the Stanton number corresponding to zero injection. This coordinate system tends to generalize results for a wide range of Reynolds number, Mach number, and nonisothermal wall conditions.

The data obtained from the present investigation is shown in Fig. 10 in terms of these parameters. Also included are theoretical [12] curves for injection of H_e and H_2. Although the data and theory are in qualitative agreement, the H_e and H_2 results do not follow clearly separated curves. It is interesting, however, that the H_e and H_2 data are separated into distinct groups if the blowing parameter is modified by multiplying it by a molecular weight ratio (M_j/M_e) or a specific heat capacity ratio (c_{pj}/c_{pe}) (Fig. 18, reference [15]).

In reviewing the plots of C_H/C_{H0} versus F/C_{H0} and (F/C_{H0})-(c_{pj}/c_{pe}) it was noted that the properties involved in C_H, C_{H0}, and F were evaluated at free-stream conditions. This raised the question of the possible effect of property variations owing to large temperature and concentration differences. It was therefore decided to consider substitution of average property values characteristic of the boundary layer.

The use of a reference state for properties evaluation in the correlation of heat and mass transfer in reactive boundary layers has recently been studied by Knuth [21, 22, 23]. By utilizing a Couette-flow model expressions for the reference temperature and composition were determined for laminar flow [21]. In a subsequent paper [22] qualitative reasoning showed that these results should be approximately valid for turbulent boundary-layer flow. The recommended relation for the reference temperature is similar to previous equations except for a term involving the wall and free-stream concentrations and the blowing rate. Calculations of reference temperatures including this term yielded values greater than the free-stream temperature for some of the injection rates. Because of this, the reference temperature was taken as the mean of the wall and free-stream values.

$$T^* = \frac{1}{2}(T_{aw} + T_w) \tag{14a}$$

Although this proved to be acceptable, it is expected that further study will lead to a more precise relation for the transpired turbulent boundary-layer reference temperature. The reference concentration recommended by Knuth was utilized. It was

$$\omega^* = 1 - \frac{M_a}{M_a - M_j} \frac{\ln \dfrac{M_e}{M_w}}{\ln \dfrac{M_e}{M_w}\dfrac{\omega_{ae}}{\omega_{aw}}} \tag{14b}$$

The heat transfer coordinates suggested herein as a result of these considerations are the ratio of the Stanton number, $C_H{}^*$, to its nonblowing counterpart, $C_{H0}{}^*$, and the blowing parameter, F^*, divided by the Stanton number for no mass transfer, $C_{H0}{}^*$, i.e.:

$$\frac{C_H{}^*}{C_{H0}{}^*} = \frac{q\rho_0{}^* c_{p0}{}^*}{q_0 \rho^* c_p{}^*}$$

$$\frac{F^*}{C_{H0}{}^*} = \frac{\rho_w v_w}{\rho^* u_e} \frac{\rho_0{}^* u_e c_{p0}{}^* (T_{aw} - T_w)}{q_0} \tag{15}$$

The success of these parameters in correlating the experimental data obtained is evident in Fig. 11. A curve representing the best fit of the data (from reference [29]) for nitrogen injection into an air stream with free-stream Mach numbers of 2.0 and 3.2 is also displayed. Additional results could not be included because the concentration levels at the wall necessary for the foregoing method of correlation were not available.

The experimental data for helium injection at an average blowing rate $F = 0.014$ and for hydrogen injection at blowing rates of $F = 0.014$ and $F = 0.0087$ fair into a single empirical curve in Fig. 11. This curve is almost exactly coincident with the nitrogen injection data of Bartle and Leadon [29] plotted in the same man-

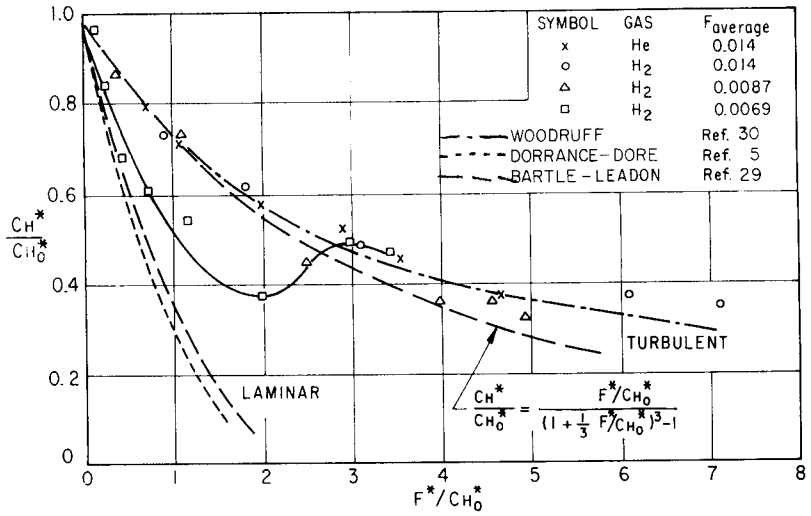

Fig. 11 General correlation of effect of gas injection on the turbulent, zero pressure gradient local heat transfer

ner. Also, it is nearly identical to the general empirical relation proposed by Bartle and Leadon for injection of air into air when it is transposed to the new set of coordinates, i.e.,

$$\frac{C_H^*}{C_{H0}^*} = \frac{F^*/C_{H0}^*}{\left(1 + \frac{1}{3} F^*/C_{H0}^*\right)^3 - 1} \tag{16}$$

It therefore appears that the proposed parameters are capable of representing the effects of such diverse molecular weight injection gases as hydrogen, helium, nitrogen, and air by one empirical curve.

The experimental data for hydrogen injection at an average blowing rate $F = 0.0069$ display the variation in Stanton number ratio one can expect when the boundary layer transforms from a laminar region through transition to a turbulent region. The heat fluxes near the leading edge of the test section asymptotically approach empirical [29] and analytical curves typical of laminar boundary layers. Only the lowest injection rate studied exhibits the transition character discussed previously. Evidently the greater mass transfer rates studied resulted in earlier destabilization of any laminar region into a turbulent boundary layer [5].

Recommended Heat Flux Prediction Procedure

On the basis of the results obtained as a consequence of this study of mass transfer into a reactive turbulent boundary layer, a specific procedure is outlined to predict heat flux rates to the wall. This procedure is fundamentally a revision of conventional incompressible relations and correction factors; however, it provides in a simple manner heat-rate distributions accurate within experimental data scatter.

The cornerstone of the technique is the calculation of the heat transfer rate under the specified free-stream conditions and wall temperature state but with no mass transfer or chemical reaction present. For wall Reynolds numbers from 10^4 to 10^7 this is given by equation (17).

$$C_{H0}{}'^* = \frac{q_{w_0}}{\rho_0^* \bar{c}_{p0}^* u_e (T_{aw} - T_w)} = 0.0291\ \mathrm{Re}_x^{*-0.2}\ \mathrm{Pr}^{*-2/3} \tag{17}$$

where all parameter properties are evaluated at the reference state defined previously.

Dissociation, recombination, and simple chemical reactions are adjusted for by a modified correction factor,

$$\frac{C_{H0}^*}{C_{H0}{}'^*} = 1 + \sum_i \frac{h_i^0\, \mathrm{Le}_i^{*2/3} (\omega_{ie} - \omega_{iw})}{\bar{c}_{p0}^* (T_{aw} - T_w)} \tag{18}$$

Finally the results from equaton (18) are corrected for the gas injection (foreign or the same as the free stream) from the curve in Fig. 11, or the empirical relation,

$$\frac{C_H^*}{C_{H0}^*} = \frac{F^*/C_{H0}^*}{\left(1 + \frac{1}{3} F^*/C_{H0}^*\right)^3 - 1} \tag{19}$$

where

$$C_H^* = \frac{q_w}{\rho^* \bar{c}_p^* u_e (T_{aw} - T_w)} \tag{20}$$

and all properties are evaluated at the reference state specified previously.

Transport properties such as viscosity, conductivity, and diffusion coefficients may be evaluated by standard techniques appropriate to multicomponent gases at high temperatures. The detailed equations derived from concepts of kinetic theory and molecular interactions and recorded by Hirschfelder, et al. [31], have been recently included on convenient monographs by Brokaw [32].

APPENDIX

Effect of Chemical Reactions on Boundary-Layer Convective Heat Transfer

Altman and Wise considered the problem of the reactive turbulent boundary layer and derived a solution based on the energy equation in terms of a temperature potential [33]. They found that a solution was possible if they assumed,

1 The longitudinal gradients in the boundary layer were small.

2 The boundary-layer thickness does not change significantly owing to chemical reaction.

3 The mole fraction of reactive species was low if more than one species was present.

4 The cold wall temperature T_w was fixed at a relatively low value by coolant flow.

5 Radiation effects and thermal diffusion could be neglected.

When the effective transport parameters were denoted by $k_{\mathrm{eff}} = k + \epsilon_k$ and $D_{i\mathrm{eff}} = D_{iM} + \epsilon_D$ the energy equation became,

$$0 = \frac{d}{dy}\left[\rho \bar{c}_p k_{\mathrm{eff}} \frac{dT}{dy} + \Sigma h_i^0 \rho D_{i\mathrm{eff}} \frac{d\omega_i}{dy}\right] \tag{21}$$

Since the values of heats of reaction are constant, an integration from $y = 0$ to $y = \delta_e$ gave

$$q_w = \rho\bar{c}_p k_{\text{eff}} \frac{dT}{dy} + \Sigma h_i^0 D_{i\text{eff}} \frac{d\omega_i}{dy} \tag{22}$$

where q_w denoted the heat flux at the wall. A second integration between $y = 0$ and $y = \delta_e$ resulted in

$$q_w = \int_0^{\delta_e} \frac{dy}{\rho\bar{c}_p k_{\text{eff}}} = T_{aw} - T_w + \sum_i \int_0^{\omega_{ie}} \frac{\rho h_i^0 D_{i\text{eff}}}{\rho\bar{c}_p k_{\text{eff}}} d\omega_i \tag{23}$$

When no recombination occurred, equation (32) reduced to

$$q_w' \int_0^{\delta_e} \frac{dy}{\rho\bar{c}_p k_{\text{eff}}} = T_{aw} - T_w \tag{24}$$

The ratio of heat flux with and without recombination for identical boundary conditions in temperature was therefore,

$$\frac{q_w}{q_w'} = 1 + \sum_i \frac{h_i^0}{(T_{aw} - T_w)} \int_0^{\omega_{ie}} \frac{\rho D_{i\text{eff}}}{\rho\bar{c}_p k_{\text{eff}}} d\omega_i \tag{25}$$

If one now introduced the concept of a reference state at which to evaluate the transport properties and assumed all $D_{i\text{eff}}$ were equal equation (25) would yield

$$\frac{q_w}{q_w'} = 1 + \Sigma \frac{h_i^0 \text{Le}^*(\omega_{ie} - \omega_{iw})}{\bar{c}_p^*(T_{aw} - T_w)} \tag{26}$$

Comparing equation (26) with experimental data in the manner of Rose, et al. [20] suggested that the Lewis number should be raised to the $^2/_3$ power; this leads to equation (10).

References

1 J. F. Gross, J. P. Hartnett, D. J. Masson, and C. Gazley, Jr., "A Review of Binary Boundary Layer Characteristics," *IJHMT*, vol. 3, 1961, p. 198.

2 H. S. Mickley, R. C. Ross, A. C. Squyers, and W. E. Stewart, "Heat, Mass and Momentum Transfer for Flow Over a Flat Plate With Blowing or Suction," NACA TN-3208, 1955.

3 B. W. Brown and P. L. Donoughe, "Tables of Exact Laminar Boundary Layer Solutions When the Wall Is Porous and Fluid Properties Are Variable," NACA TN-2479, 1951.

4 W. H. Dorrance, *Viscous Hypersonic Flow*, chapter V, McGraw-Hill Book Company, Inc., New York, N. Y., 1962.

5 W. H. Dorrance and F. J. Dore, "The Effects of Mass Transfer on the Compressible Turbulent Boundary Layer Skin Friction and Heat Transfer," *Journal Aeronaut. Sci.*, vol. 21, 1954, p. 404.

6 M. W. Rubesin, "An Analytical Estimation of the Effect of Transpiration Cooling on the Heat-Transfer and Skin-Friction Characteristics of a Compressible, Turbulent Boundary Layer," NACA TN-3341, 1954.

7 W. E. Brunk, "Experimental Investigation of Transpiration Cooling for a Turbulent Boundary Layer in Subsonic Flow Using Air as a Coolant," NACA TN-4091, 1957.

8 E. R. G. Eckert, P. J. Schneider, A. A. Hayday, and R. M. Larson, "Mass Transfer Cooling of a Laminar Boundary Layer by Injection of a Lightweight Foreign Gas," *Jet Propulsion*, vol. 28, 1958, p. 34.

9 E. R. Van Driest, "On the Mass Transfer Near the Stagnation Point," RAND Symposium on Mass Transfer Cooling for Hypersonic Flight, June, 1957.

10 M. R. Denison, "The Turbulent Boundary Layer on Chemically Active Ablating Surfaces," *Journal of Aeronaut. Sci.*, vol. 28, 1961, p. 271.

11 N. Ness, "Foreign Gas Injection Into a Compressible Turbulent Boundary Layer on a Flat Plate," *Journal of Aeronaut. Sci.*, vol. 28, 1961, p. 645.

12 M. W. Rubesin and C. C. Pappas, "An Analysis of the Turbulent Boundary Layer Characteristics on a Flat Plate With Distributed Foreign Gas Injection," NACA TN-4149, 1958.

13 P. A. Libby and M. Pieruci, "Laminar Boundary Layer With Hydrogen Injection Including Multicomponent Diffusion," *AIAA Journal*, vol. 2, 1954, p. 2118.

14 A. N. Tifford, "On Surface Mass Transfer Effects in a Binary Fluid," Aeronautical Res. Labs. Report ARL-62-396, 1962, *AIAA Journal*, vol. 1, 1963, p. 1414.

15 R. N. Meroney, "Experimental Investigation of the Effects of Transpiration Cooling on a Partially Dissociated Turbulent Boundary Layer," Univ. of Calif., Berkeley, Engr. Proj. Report AS-63-6, 1963.

16 P. L. Donoughe and R. A. McKinnon, "Experimental Investigation of Air Flow Uniformity and Pressure Level on Wire Cloth for Transpiration-Cooling Applications," NACA TN-3652, 1956.

17 "Table IIIC, Specific Heats of High Alloy Steels," *Physical Constants of Some Commercial Steels at Elevated Temperatures*, Butterworth Scientific Publications, London, 1953.

18 E. R. G. Eckert, J. P. Hartnett, and T. F. Irvine, Jr., "Measurement of Total Emissivity of Porous Materials in Use for Transpiration Cooling," *Jet Propulsion*, vol. 26, 1956, p. 280.

19 E. J. Russ, "Heating Rate Characteristics of an Oxyacetylene Flame Apparatus for Surface Ablation Studies," Univ. of Calif., Inst. Engr. Res. Report HE-150-176, Berkeley, 1959.

20 P. H. Rose, R. F. Probstein, and Mac C. Adams, "Turbulent Heat Transfer Through a Highly Cooled, Partially Dissociated Boundary Layer," *Journal of Aeronaut. Sci.*, vol. 25, 1958, p. 751.

21 E. L. Knuth, "Use of Reference States and Constant Property Solutions in Predicting Mass-, Momentum-, and Energy-Transfer Rates in High Speed Laminar Flows," *LJHMT*, vol. 6, 1963, p. 2.

22 E. L. Knuth and H. Dershin, "Use of Reference States in Predicting Transport Rates in High-Speed Turbulent Flows With Mass Transfers," *IJHMT*, vol. 6, 1963, p. 999.

23 E. L. Knuth, "A Preliminary Study on the Use of Reference States in Predicting Transport Rates in Flows With Chemical Reactions," *IJHMT*, vol. 6, 1963, p. 1083.

24 G. A. Marxmann and M. Gilbert, "Turbulent Boundary Layer Combustion in the Hybrid Rocket," *Ninth Symposium on Combustion*, Academic Press, New York, N. Y., 1963, 371ff.

25 F. E. C. Culick, "The Equations of Conservation for Multicomponent Reacting Gas Flows," M.I.T. Aerophysics Lab. Tech. Report 48, 1962.

26 P. N. Romanenko and V. N. Kharchenko, "The Effect of Transverse Mass Flow on Heat Transfer and Friction Drag in a Turbulent Flow of Compressible Gas Along an Arbitrarily Shaped Surface," *IJHMT*, vol. 6, 1963, p. 727.

27 C. J. Scott, G. E. Anderson, and D. R. Elgin, "Laminar, Transitional, and Turbulent Mass Transfer Cooling Experiments at Mach Numbers From 3 to 5," Inst. of Tech., Univ. of Minn., Research Report 162, AFOSR TN 59-1305, 1959.

28 J. P. Hartnett, J. F. Gross, and Carl Gazley, "Mass-Transfer Cooling in a Turbulent Boundary Layer," *Journal Aeronaut. Sci.*, vol. 27, 1960, p. 623.

29 E. R. Bartle and B. M. Leadon, "Mass Transfer Cooling on a Turbulent Boundary Layer," *Proceedings of HTFMI*, Stanford University Press, vol. 27, 1962.

30 L. W. Woodruff, (Untitled Report), Boeing Aircraft Co., Seattle, Wash., Report D2-2202, 1962.

31 J. O. Hirschfelder, C. F. Curtiss, and R. B. Bird, *Molecular Theory of Gases*, John Wiley & Sons, Inc., New York, N. Y., 1954.

32 R. S. Brokaw, "Alignment Charts for Transport Properties Viscosity, Thermal Conductivity, and Diffusion Coefficients for Non-polar Gases and Gas Mixtures at Low Densities," NASA TR R-81, 1961.

33 D. Altman and H. Wise, "Effect of Chemical Reactions in the Boundary Layer on Convective Heat Transfer," *Jet Propulsion*, vol. 26, 1956, p. 256.

34 S. R. Brinkley, H. E. Edwards, and R. W. Smith, "The Thermodynamics of Combustion Gases," *Bureau of Mines Report 4958*, 1953.

Printed in U. S. A.

Keep - Bobs Paper (Ph.D. Theses)